ELSEVIER

Journal of Power Sources 55 (1995) 231–236

JOURNAL OF POWER SOURCES

Cycle analyses of thermoelectric power generation and heat pumps using the β''-alumina electrolyte

Kazuo Onda, Toshihisa Masuda, Susumu Nagata, Ken Nozaki

Electrotechnical Laboratory, 1-1-4 Umezono, Tsukuba, Ibaraki 305, Japan

Received 7 January 1995; accepted 8 February 1995

Abstract

Cycle analyses of the alkali-metal thermoelectric conversion (AMTEC) and the high-temperature heat pump using the β''-alumina electrolyte was performed. It is shown that the isothermal expansion or compression of the sodium ion flow through the electrolyte coincides with the expansion or compression process in the Ericsson cycle, respectively, when the internal losses by thin electrolyte and electrodes are small. The isothermal compression approximation in the heat-pump cycle is more consistent with the isothermal expansion in the AMTEC cycle than the adiabatic compression discussed in an earlier report. Typical voltage–current characteristics and thermal efficiencies for both the AMTEC and the heat pump are presented including not only the saturated liquid case, but also the superheated vapour case of sodium at the high temperature side. The operation in superheated vapour shows a decrease in the power-generation efficiency for the AMTEC and an increase in the coefficient of performance for the heat pump.

Keywords: Thermoelectricity; Heat pumps; Alumina electrolyte

1. Introduction

The β''-alumina solid electrolyte (BASE) is a sodium ion conductor. When a sodium pressure difference is made across the electrolyte, Na^+ ions can flow from the high pressure side to the low pressure side through the electrolyte. Also, Na^+ ions are forced to move by an external electric source applied to the electrolyte. A neutral sodium atom cannot flow into the electrolyte as an ion unless the atom emits an electron into the outer circuit at the electrolyte surface, and the ion cannot get out of the electrolyte as a neutral atom unless the ion captures an electron via the outer circuit. When a temperature difference is made across the electrolyte to produce a pressure difference, a device for thermoelectric power generation can be formed where thermal energy is converted directly to electricity. This is called the alkali-metal thermoelectric conversion (AMTEC) or the sodium heat engine (SHE), which was experimentally demonstrated and patented by Kummer and Weber [1]. The underlying principle of the AMTEC is illustrated in Fig. 1. Recently, many research groups have developed the AMTEC as a possible high-reliability power source without any moving parts, with a high efficiency (20 to about 40%), little scalability, and easy stacking of cell module with high-power density

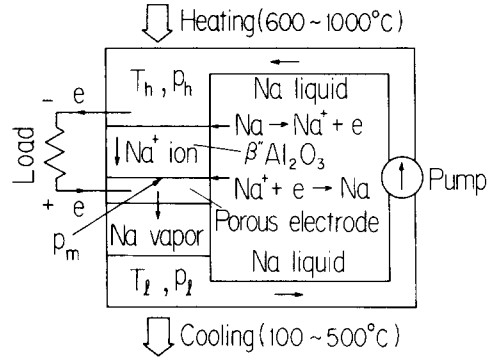

Fig. 1. Schematic diagram of alkali-metal thermoelectric conversion.

[2–10]. The space applications of AMTEC, in particular, have received much attention [7,9].

A high-temperature sodium heat pump was proposed by Jeter [11], where the electrolyte works as a compressor of sodium from a low-pressure side to a high-pressure side driven by an external source. A sodium/sulfur battery is charged by an external source to separate sodium from Na_2S_x through the electrolyte. Electric power is discharged to the outer circuit by returning the separated sodium through the electrolyte under the action of a difference in Gibbs free energy (ΔG). This means the electrolyte can work as both a compressor

SSDI 0378-7753(95)02194-L

and a turbine. The electrothermal operation of the electrolyte as a turbine or a compressor corresponds to the AMTEC or heat-pump cycle.

It is desirable to keep the electrolyte temperature as high as possible to minimize the internal loss because the ionic resistance of the electrolyte decreases as the temperature increases. The AMTEC process has been analysed hitherto under the assumption that isothermal expansion was held at the temperature of the high-temperature side, and the analysis agrees well with the experimental results [3,4,6,8]. Parenthetically, the isothermal expansion is the same as the expansion process in the Ericsson cycle. To our knowledge, this is the first report that discusses the similarity between these two processes. In previous cycle analyses of the high-temperature sodium heat pump [11] the expansion process was taken, as an approximation, to be adiabatic. In this report, this adiabatic expansion process is also discussed in comparison with the isothermal expansion in the Ericsson cycle to clarify the heat-pump performance.

Most AMTEC experiments have been performed under the condition where the high-temperature side of the electrolyte contacts with saturated sodium liquid, which can also act as the electrode for the high-temperature side. A practical AMTEC device must have each cell connected in series because the output voltage from each cell is of the order of 1 V. One of the technical concerns is to avoid shorting the series connection by supplying liquid sodium to each cell. The AMTEC device can work even when sodium is supplied as a vapour instead of as a liquid. Indeed, by using the vapour it is much easier to avoid the electrical shorting that occurs when using liquid sodium [12,13]. In this report, the cycle performances of AMTEC and heat pump are estimated under a superheated condition.

2. Cycle analyses of thermoelectric power generation and heat pump

2.1. Voltage–current characteristics for AMTEC

Before proceeding to cycle analysis, the basic equations to describe the voltage–current characteristics for AMTEC are introduced first. The ΔG for sodium across the electrolyte is the thermodynamic driving force for sodium ions, and the open-circuit voltage, V, for such a concentration cell of AMTEC is given as follows [6]:

$$\Delta V = -\frac{\Delta G}{F} = -\frac{\Delta(H-TS)}{F} = \frac{-v\Delta p + S\Delta T}{F} \quad (1)$$

where F is the Faraday constant, H the enthalpy, T the temperature, S the entropy, v the specific volume, and p the pressure. When the electrolyte for the concentration cell is kept at the temperature of the high-temperature side, T_h, Eq. (1) can be rewritten as follows, assuming that sodium is an ideal gas:

$$\Delta V = v\Delta p/F = -(RT_h/F)(\Delta p/p) \quad (2)$$

where R is the gas constant. Integration of Eq. (2) from p_h of the high-pressure side to an intermediate pressure, p_m, gives:

$$V = (RT_h/F)\ \ln(p_h/p_m) \quad (3)$$

When the electric circuit is open, the molecular flow rate of sodium, $\dot{n}_m$, from the electrolyte surface of the low-pressure side kept at pressure p_m becomes equal to the molecular flow rate of sodium, $\dot{n}_l$, from the condensing surface kept at temperature, T_l. This results in no net transfer of sodium [6], i.e.:

$$\dot{n}_m = \frac{p_m}{\sqrt{2\pi MRT_h}} = \frac{p_l}{\sqrt{2\pi MRT_l}} = \dot{n}_l \quad (4)$$

where M is the atomic weight of sodium. Eliminating p_m in Eq. (3) by Eq. (4), the open-circuit voltage is rewritten as:

$$V = (RT_h/F)\ \ln[p_h/(p_l\sqrt{T_h/T_l})] \quad (5)$$

Next, we deal with the case for current flowing through an outer load. When there is a net flow rate of sodium ion, $\dot{n}_i$, it is related with the current density i as follows:

$$i = \dot{n}_i F \quad (6)$$

If the high-pressure side is kept at a constant pressure, p_h, then the electrolyte surface pressure on the low-pressure side increases from the equilibrium pressure, $p_l\sqrt{T_h/T_l}$, by the amount of the pressure p_m that corresponds to $\dot{n}_i$ in Eq. (4). This means that the following well-known equation for the voltage–current characteristics can be introduced:

$$V = \frac{RT_h}{F}\ln\frac{p_h}{p_l\sqrt{T_h/T_l} + \sqrt{2\pi MRT_h}\,i/F} - iR_O$$
$$= (RT_h/F)\ \ln(p_h/p_m) - iR_O \quad (7)$$

where p_m represents the pressure at the electrolyte surface of the low-pressure side. The last term, R_O, in the right-hand side of Eq. (7) is the ohmic resistance for both the ionic and the electric conductors of the electrolyte and the electrodes, respectively. Usually, the ohmic loss is designed to be smaller in the electrodes than in the electrolyte. Other losses due to electrode activation, gas diffusion, etc., are neglected for simplicity. Experimental voltage–current characteristics obtained hitherto can be described well by Eq. (7).

The voltage–current characteristics for thermoelectric power generation, Eqs. (6) and (7) can be easily applied to the heat-pump cycle when the signs for both $\dot{n}_i$ and i become negative. This means that Na^+ ions are forced to flow, as opposed to the case of power generation,

from the low-pressure side to the high-pressure side by an external source instead of by an external load. The performance of the compressor can be described by Eqs. (6) and (7) by keeping the pressure of the high-pressure side constant and by keeping the temperature of the electrolyte constant at T_h. The following condition for the current density, i, must be satisfied, however, so that p_m in Eq. (7) is kept positive:

$$p_l\sqrt{T_h/T_l}+\sqrt{2\pi MRT_h}\,i/F>0 \tag{8}$$

As shown in Eq. (7) above, the electrolyte temperature should be kept sufficiently high so that the internal resistance decreases to minimize the internal loss. In this sense, it is a better operation for a compression process by the electrolyte to keep the whole electrolyte temperature at a high isothermal temperature such as in the AMTEC cycle, rather than by assuming an adiabatic compression as proposed by Jeter [11]. Furthermore, the high-pressure side is not necessarily filled with the saturated liquid. Instead, superheated sodium gas can be introduced when another porous electrode is provided at the high-temperature side of the electrolyte. In this case, the resistance for another electrode must be included in the R_O term of Eq. (7).

2.2. Similarity of AMTEC cycle with Ericsson cycle

Up to now, many studies on the power-generation efficiency of the AMTEC cycle have been presented [2–10], but the similarity of the AMTEC cycle with the Ericsson cycle has not been discussed. The isothermal expansion is an expansion process of the Ericsson cycle where the work done externally is equal to the heat supplied during the process. The external work, W_{out}, and the heat input, Q_{in}, in the Ericsson cycle for molecular flow rate, $\dot{n}$, can be described as follows:

$$W_{out}=\int_h^m \dot{n}p\,dv=\dot{n}RT_h\ln\frac{p_h}{p_m}=Q_{in} \tag{9}$$

When the internal resistance, R_O, is sufficiently small to be neglected, the output voltage, V, in Eq. (7) can be approximated by:

$$V=(RT_h/F)\ln(p_h/p_m) \tag{10}$$

The electrical output, W_{out}, for AMTEC is obtained by multiplying the current density, i, in Eq. (6) with the above voltage V, i.e.:

$$W_{out}=Vi=\dot{n}_iRT_h\ln(p_h/p_m) \tag{11}$$

This means that the power-generation process in the AMTEC cycle can be well approximated by the isothermal expansion process in the Ericsson cycle. It is also found that the same amount of heat input as electric output is required during the power-generation process.

A schematic diagram of the AMTEC cycle is given in Fig. 2. The AMTEC cycle can be indicated in the temperature–entropy (T–S) diagram of Fig. 3 because the isothermal expansion of the AMTEC cycle can be approximated by the expansion process in the Ericsson cycle. Fig. 3 shows a case where the high-temperature side is filled with saturated sodium liquid.

The efficiency of power generation, η_{gen}, is given similarly to previous studies as follows:

$$\eta_{gen}=W_{out}/[W_{out}+(L+\Delta H)\dot{n}_i+W_{pump}+K(T_h-T_l)+(\sigma/Z)(T_h^4-T_l^4)] \tag{12}$$

where L is the latent heat for vaporization, ΔH the sensible heat from the pump-outlet temperature to T_h, and power output per unit area of electrolyte, W_{out}, is given by Eqs. (6) and (7) as follows:

$$W_{out}=\dot{n}_iRT_h\ln(p_h/p_m)-(\dot{n}_iF)^2R_O \tag{13}$$

where W_{pump} is the pump power required to drive an $\dot{n}_i$ molecular flow rate of liquid sodium from p_l to p_h and it is usually negligible compared with W_{out}. The fourth and fifth term in the denominator of Eq. (12) represent heat conduction and radiation losses, respectively, where K is a coefficient for heat-conduction loss, Z a coefficient for heat-radiation loss, and σ the Stefan–Boltzmann constant. In the denominator of Eq. (12) W_{out} is involved because the power-generation process of the Ericsson cycle needs the same amount

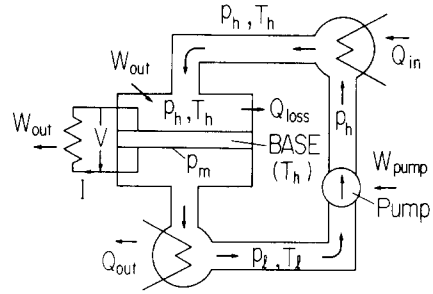

Fig. 2. Cycle diagram of alkali-metal thermoelectric conversion.

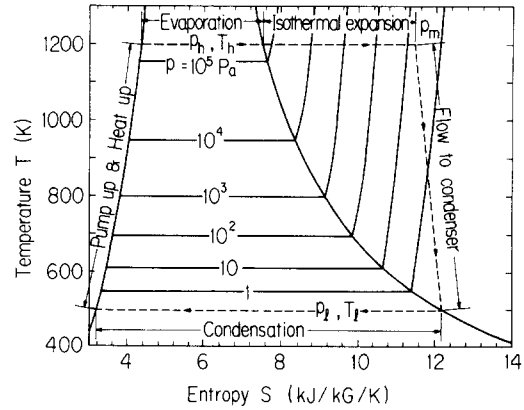

Fig. 3. Temperature vs. entropy diagram of alkali-metal thermoelectric conversion.

of heat input as power output, as described earlier. In Eq. (13) W_{out} is different from the ideal power output in the isothermal expansion process of the Ericsson cycle by the amount of internal loss by ohmic heating, resulting in reduced W_{out} and Q_{in}. However, the ohmic heating in the electrolyte causes the electrolyte temperature to remain constant or increase.

2.3. Heat-pump cycle

The coefficient of performance (*COP*) of the high-temperature sodium heat pump proposed by Jeter [11] is calculated assuming an adiabatic compression of sodium vapour through the electrolyte. The compression process is more reasonably approximated, however, by the isothermal process as described above. In this report, the *COP* of the heat pump cycle is calculated under the condition of the same isothermal compression as the Ericsson cycle.

A schematic diagram of the heat-pump cycle using the electrolyte is shown in Fig. 4, and the *T–S* diagram in the case of saturated liquid in the high-temperature side is presented in Fig. 5. As in the AMTEC cycle, a porous and thin electrode is required at the low-pressure side of BASE. Sodium liquid can function as an electrode when the high-temperature side is filled with saturated liquid, but another porous and thin electrode is needed when a superheated vapour is introduced in the high-temperature side, as in the AMTEC cycle.

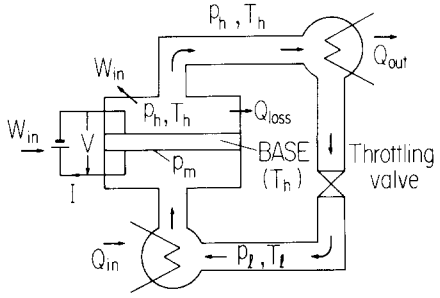

Fig. 4. Cycle diagram of solid electrolyte heat pump.

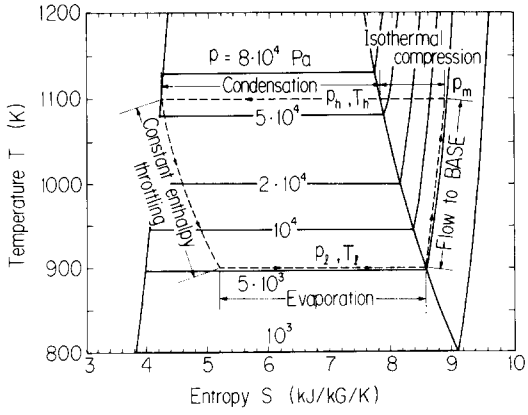

Fig. 5. Temperature vs. entropy diagram of solid electrolyte heat pump.

The *COP* of the heat pump is defined as the ratio of heat pumped to the high-temperature side of T_h or T_h' (superheated temperature) minus heat losses to the low-temperature side (T_l) divided by the compressor power $|W_{in}|$ (W_{in} is negative due to the negative ri) as follows:

$$COP = \{|W_{in}| + (L + \Delta H_s - \Delta H)|ri| - K(T_h - T_l) - (\sigma/Z)(T_h^4 - T_l^4)\}/|W_{in}| \quad (14)$$

where ΔH_s is the sensible heat cooled down from the superheated to saturated temperatures, ΔH the sensible heat warmed up from T_l to T_h, and the third and the fourth terms in the numerator represent the heat conductive and radiative losses, respectively. $|W_{in}|$ in the numerator of Eq. (14) is required because the same heat as the compression power $|W_{in}|$ is rejected to the high-temperature side in the isothermal compression process of the Ericsson cycle in a similar fashion to the AMTEC cycle. ΔH can be reduced by recovering a part of the conductive and radiative heat losses, but it is not considered here. The consumed power per a unit area of electrolyte as a compressor is represented as follows as in Eq. (13):

$$W_{in} = ri RT_h \ln(p_h/p_m) - (ri F)^2 R_O \quad (15)$$

where the signs for i and ri are negative, in contrast with the AMTEC cycle because current must be supplied from an external source and this results in a negative W_{in}.

By substituting Eq. (15) in Eq. (14), the *COP* can be rewritten as:

$$COP = [RT_h \ln(p_h/p_m) + (|ri|F)^2 R_O + (L + \Delta H_s - \Delta H) - K(T_h - T_l)/|ri| - (\sigma/Z)(T_h^4 - T_l^4)/|ri|] / [RT_h \ln(p_h/p_m) + (|ri|F)^2 R_O] \quad (16)$$

The heat loss, except to the low-temperature side (T_l), is not considered in both AMTEC and heat-pump cycles. When the heat loss to the surrounding atmosphere is lower than T_l, it must be accounted for in the calculation in order to obtain more realistic results.

3. Results and discussion

The thermal properties of sodium by Ohse [14] are adopted in this work and the ionic resistivity ρ_{BASE} of the electrolyte is given by:

$$\rho_{BASE} = T[4.03 \times 10^{-4} \exp(1420/T) + 1.68 \times 10^{-7} \exp(5567/T)] \quad (\Omega\ \mathrm{m}) \quad (17)$$

Molybdenum shows good durability in a sodium atmosphere when serving as porous and thin electrodes.

The following specific resistivity for solid molybdenum [15] is used because reliable measured properties for porous electrodes have not been reported:

$$\rho_{Mo}=5.6\times10^{-8}[1+4.4\times10^{-3}(T-293)] \quad (\Omega\ m) \quad (18)$$

The thicknesses of the electrolyte and the electrode were set at 1 mm and 3 μm, respectively, according to the previous AMTEC reports on cell structure, electrical resistivity and sodium vapour permeability through electrodes. The cell configurations, such as the power leads and the radiation shield, are designed to reduce heat loss. The optimum configuration gives a conduction and a radiation loss of 0.378 and 2.28 W/cm^2, respectively, when $T_h=1200$ K and $T_l=500$ K. The efficiency of the liquid sodium pump is assumed to be 10% and this corresponds to a typical value for a small unit. W_{pump} is negligible small when compared with W_{out}.

3.1. AMTEC cycle analysis

The voltage–current characteristics and the η_{gen} related with i for $T_h=1200$ K and $T_l=500$ K are given in Fig. 6, including the superheated condition. The AMTEC operation at $T_h=1200$ K is thought to be soon attained because the 100 W power-generation test at $T_h=1073$ K was performed for more than 1500 h [9]. Three cases are shown in Fig. 6, namely two saturated liquid cases of $T_h=1200$ and 1100 K, and a superheat case of $T_h=1200$ K (the corresponding saturated temperature $T_h'=1100$ K). The three cycles that give the maximum η_{gen} in Fig. 6 are shown in the T–S diagram of Fig. 7.

The maximum efficiencies of power generation for the three cases (i.e., saturated liquid of $T_h=1200$ K, saturated liquid of $T_h=1100$ K, and superheated vapour of $T_h=1200$ K) are 21.8, 20.6 and 19.1%, respectively. The saturated liquid case has a higher efficiency than the superheated vapour counterpart for the same temperature ($T_h=1200$ K) because the former has a higher pressure p_h than the latter, resulting in the larger W_{out} (see Eq. (9)). The saturated liquid case of $T_h=1100$ K has a higher efficiency than the superheated vapour case of $T_h=1200$ K because the increase in ΔH and heat losses due to the temperature increase in the denominator of Eq. (12) are larger than the increase in power output, W_{out}. The calculated example suggests that a higher efficiency might be obtained at the minimal temperature increase for superheating which is preferable for the electrical insulation in a series connection, even though heat losses are variable and depend on the cell design.

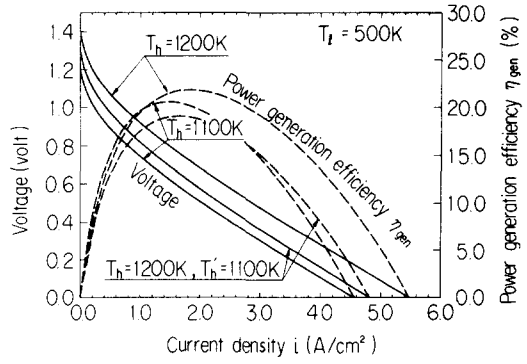

Fig. 6. Voltage–current characteristics and relation between η_{gen} and i of thermoelectric power generation.

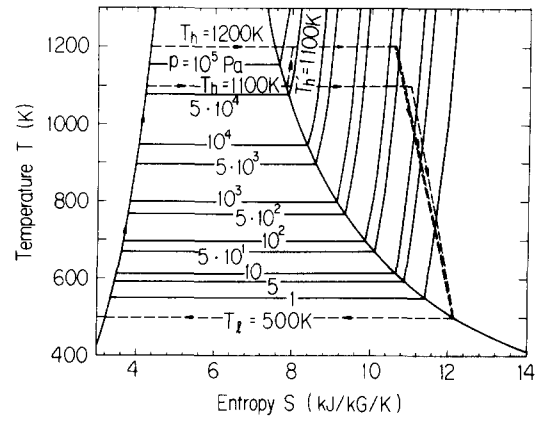

Fig. 7. Temperature vs. entropy diagram of thermoelectric power generation for saturated liquid and superheated vapour.

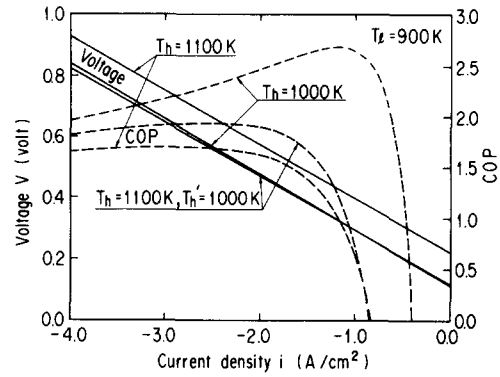

Fig. 8. Voltage–current characteristics and relation between coefficient of performance (*COP*) and i of solid electrolyte heat pump.

3.2. Heat-pump cycle analysis

The heat pump using electrolyte can be employed at higher temperatures than conventional heat pumps. As typical examples, the voltage–current characteristics and the *COP* related with current are shown in Fig. 8 for the saturated liquid cases $T_h=1100$ and 1000 K, together with a superheated case for $T_h=1100$ K (the corresponding saturated temperature is $T_h'=1000$ K). The voltage–current characteristics for a saturated liquid when $T_h=1000$ K almost coincide with those for superheated vapour ($T_h=1100$ K) because of a cancellation of an increase in the first term in the right-hand side of Eq. (7) by a high temperature T_h and a decrease in the second term of internal loss $-iR_O$ in Eq. (7)

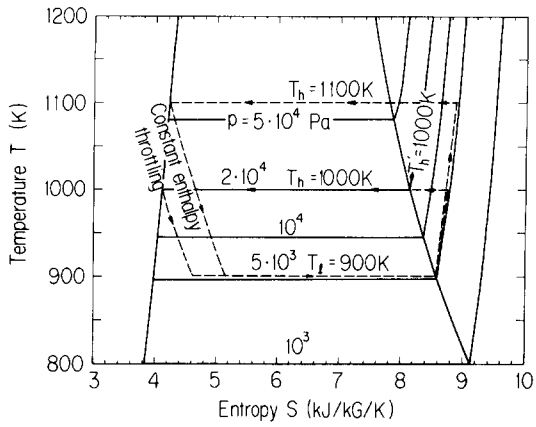

Fig. 9. Temperature vs. entropy diagram of heat pump for saturated liquid and superheated vapour.

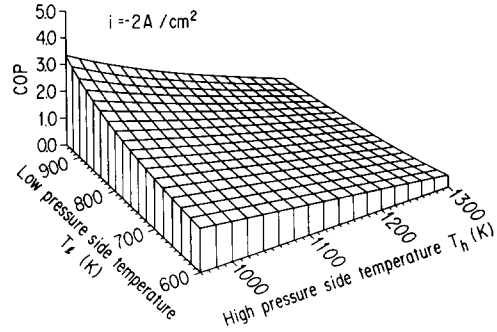

Fig. 10. Variation of coefficient of performance (*COP*) for temperature change of high-pressure side T_h and low-pressure side T_l in heat-pump cycle.

by lowering resistance R_O for high temperature, where $-iR_O$ is positive because i is negative for a heat-pump cycle. The *COP* for $T_h = 1000$ K is higher than that for $T_h = 1100$ K of a saturated liquid because the heat loss for the latter is higher than that for the former and the W_{in} and $\Delta H_s - \Delta H$ terms in Eq. (14) are almost the same in both cases. The superheated case has a higher *COP* than the saturated case for $T_h = 1100$ K, because the former has a larger $|W_{in}|$ and a smaller $L_l + \Delta H_s - \Delta H$ than the latter. The superheated condition in the heat-pump cycle gives a good result in reverse to the power-generation cycle at the same temperature.

The *COP* increases as the current decreases and reaches at maximum at $i = 0$ when there is no heat loss according to Eq. (16), but no heat is pumped up at $i = 0$. In a real cycle, the maximum *COP* is obtained at $i = -1$ to about -3 A/cm^2 because the ratio of heat loss to pumped-up heat decreases as i increases.

Three cycles which give the maximum *COP* in Fig. 8 are shown in the *T–S* diagram of Fig. 9. The low temperature T_l which satisfies Eq. (8) at $i = -1$ to about -3 A/cm^2 is 579–612 K, so the operating temperature of T_l is supposed to be above 580 K in a heat-pump cycle when BASE is used. Fixing $i = -2$ A/cm^2, the variation of *COP* is shown in Fig. 10 in the range of T_h from 960 to 1300 K and T_l from 600 to 940 K. The *COP* of this heat pump shows the same tendency as a conventional one in that it increases when T_l approaches T_h (but T_l must be less than T_h).

4. Conclusions

In the cycle analyses of alkali-metal thermoelectric conversion and a high-temperature heat pump using β''-alumina solid electrolyte, it is shown that the expansion or compression process of sodium ion flow through the electrolyte is equivalent to the isothermal expansion or compression process in the Ericsson cycle when the internal loss through the concentration cell is small. Moreover, the isothermal compression process in the heat-pump cycle is more consistent with the AMTEC cycle than the adiabatic compression process reported previously. Typical cycle analyses of AMTEC and a high-temperature heat pump, taking into account heat loss, have been performed to obtain their voltage–current characteristics and thermal efficiency for both a saturated liquid and a superheated vapour at the high-temperature side of the cycle. The superheating condition decreases the power-generation efficiency in the AMTEC cycle, but it increases the coefficient of performance in the heat-pump cycle.

References

[1] J.T. Kummer and N. Weber, *US Patent No. 3 458 356* (1969).
[2] N. Weber, *Energy Convers., 14* (1974) 1.
[3] T.K. Hunt, N. Weber and T. Cole, *Proc. 13th Intersociety Energy Conversion Engineering Conf., San Diego, CA, USA, 1978,* Vol. 3, p. 2011.
[4] T.K. Hunt, N. Weber and T. Cole, *Solid State Ionics, 5* (1981) 263.
[5] T. Cole, *Proc. Workshop Thermally Regenerative Electrochemical Systems, SERI/CP-234-1577 (1981) 109,* Solar Energy Research Institute, Goldon, CO, USA.
[6] T.K. Hunt and N. Weber, Research and development on a sodium heat engine, US Department of Energy, *Final Rep. DOE/ER/10347-T1,* 1982.
[7] C.P. Bankston, T. Cole, R. Jones and R. Ewell, *J. Energy, 7* (1983) 442.
[8] T. Cole, *Science, 221* (1983) 915.
[9] J.V. Lasecki, R.F. Novak, J.R. McBride, J.T. Brockway and T.K. Hunt, *Proc. 22th Intersociety Energy Conversion Engineering Conf., Philadelphia, PA, USA, 1987,* Vol. 3, p. 1408.
[10] T. Masuda, K. Tanaka, A. Negishi and T. Honda, *Proc. 23th Intersociety Energy Conversion Engineering Conf., Denver, 1988,* Vol. 1, p. 347.
[11] S.M. Jeter, *Energy, 12* (1987) 163.
[12] R.K. Sievers, R.A. Markley, J.E. Schmidt, N. Weber, J.R. Rasmussen, S. Olsen and T.K. Hunt, *5th Symp. Space Nuclear Power Systems, Albuquerque, NM, USA, 1988,* p. 615.
[13] R.F. Novak, J.R. McBride and T.K. Hunt, *5th Symp. Space Nuclear Power Systems, Albuquerque, NM, USA, 1988,* p. 625.
[14] R.W. Ohse, *Handbook of Thermodynamic and Transport Properties of Alkali Metals,* Blackwell, Oxford, 1985, p. 547.
[15] Tokyo Astronomical Observatory (ed.), *Chronological Scientific Tables,* Maruzen, 1985, Nihonbashi, Tokyo, p. 519.